scientific reports

Check for updates

OPEN

MiR-27a-3p protects against $NaAsO_2$-induced neuronal apoptosis in HT22 cells

Qiyao Zhang[1,3], Siqi Zhao[1,3], Teng Ma[1], Yujie Wang[1], Shiqing Xu[1], Suhua Wang[2], Xiaohui Wang[1]✉ & Li Wang[1]✉

Environmental arsenic exposure is closely related to nerve damage. Recent research suggests miR-27a-3p is involved in the development of certain neurodegenerative and neuropsychiatric diseases. Nonetheless, the precise impact of miR-27a-3p on neuron functioning in the hippocampus remains unclear. In this investigation, models were established using $NaAsO_2$-treated mice and cells to investigate this aspect. Male C57BL/6J mice were given drinking water containing sodium arsenite (0, 0.5, 5, or 50 ppm) for 48 weeks. The results showed that sodium arsenite induced apoptosis in mouse neurons. After 6 μmol/L sodium arsenite treatment in HT22 cells, miR-27a-3p expression level was decreased, FTO, DRP1 and p-DRP1 (Ser616), neuronal apoptosis and pro-apoptotic proteins (Bax and cleaved asparaginase 3) were increased, and anti-apoptosis proteins Bcl-2 and MMP were decreased, which indicated that sodium arsenite could activate FTO/DRP1 pathway. Furthermore the process could be reversed by miR-27a-3p mimics. This study demonstrates that miR-27a-3p alleviates sodium arsenite-induced mitochondrial dysfunction and apoptosis in HT22 cells by inhibiting the FTO/DRP1 pathway. This study provides a scientific basis for finding early biomarkers for the control of arsenic-induced neurotoxicity and discovering new prevention and control measures.

Keywords miR-27a-3p, Arsenic, Apoptosis, Hippocampus

Arsenic is a global health concern and environmental contaminant, with its toxicity impacting millions of individuals worldwide[1]. miR-27a-3p is capable of ameliorating brain diseases produced by $NaAsO_2$ accumulation and toxicity[2,3]. However, the specific underlying mechanisms remain unclear. Currently, drug and surgical treatments for neurological impairment have limited efficacy, underscoring the urgent need for novel therapeutic strategies.

MicroRNA (miRNA) is a class of noncoding RNA influencing the progression of various disorders, including neurological disorders[4,5]. Expression of miRNA abnormalities in the hippocampus has been associated with neurodegenerative disorders characterized by apoptosis[6]. The miR-27 gene family encompasses two similar members, miR-27a and miR-27b, widely distributed in vertebrates[7]. Previous studies have shown that miR-27a-3p can promote apoptosis in certain contexts[8]. The role of miR-27a-3p in neurodegenerative diseases remains controversial. For instance, its overexpression has been shown to alleviate cerebral ischemia–reperfusion injury[9], whereas its downregulation can mitigate the neurotoxicity induced by sevoflurane[10]. HT22 cells undergoing Oxygen Glucose Deprivation/Reperfusion (OGD/R)-induced apoptosis displayed significant downregulation of miR-27a-3p[11]. However, its biological role in neurological impairme nt or apoptosis remains elusive. Notably, downregulation of miR-27a-3p was identified during OGD/R-associated HT22 apoptosis, while miR-27a-3p overexpression overturned the OGD related apoptosis in HT22 cells. Moreover, dosing with a miR-27a-3p agomir significantly limited TUNEL positivity following cerebral ischemia/reperfusion injury (CI/R) utilizing an in vivo rat model[12]. Several neurological diseases may benefit from miR-27a-3p as a therapeutic approach. However, contradictions have been identified; for instance, downregulating miR-27a-3p levels improved sevoflurane-associated neurotoxicity and neuroplasticity[10]. This discrepancy spurred further examination of the regulatory role of miR-27a-3p on neuronal function.

The hippocampus is a vital area of the brain that performs essential functions in memory formation, learning, controlling emotions, and perceiving pain. The link between mitochondrial dysfunction and hippocampal neuronal damage has been investigated recently[13,14]. Mitochondrial membrane potential (MMP) is an early and critical indicator of apoptosis. SH-SY5Y cells exposed to As_2O_3 alone exhibit a significant reduction in MMP,

[1]School of Public Health, Baotou Medical College, Baotou 014040, Inner Mongolia, China. [2]Ulanqab Medical College, Baotou 012000, Inner Mongolia, China. [3]Qiyao Zhang and Siqi Zhao contributed equally. ✉email: 102018909@btmc.edu.cn; 101995002@btmc.edu.cn

suggesting mitochondrial dysfunction[15]. Fat mass and obesity-associated protein (FTO), widely expressed in nervous tissue, regulates mitochondria-mediated apoptosis[16]. FTO-mediated FTO/DRP1 signaling contributes to apoptosis[17]. Through the analysis of bioinformatics data, it has been discovered that miR-27a-3p operates as a suppressor of cancer progression in glioma. This is achieved by directly binding to FTO, which results in the inhibition of its expression[18].

However, the exact link between miR-27a-3p and FTO in arsenic-induced nerve injury and apoptosis remains uncertain. HT22 cells are often used as an in vitro model to study neuroinflammation and cell signaling pathways. Therefore, we explored the role of miR-27a-3p in the process of arsenic exposure-induced neurological injury by establishing HT22 cell models and animal models, aiming to provide new ideas for the discovery of new biomarkers of health damage caused by arsenic exposure.

Materials and methods

Mice and experimental groups

Male C57BL/6J mice aged five weeks were obtained from Calvin Biotechnology Co., Ltd. (Inner Mongolia, China). Experimental treatments received approval from the Experimental Animal Ethics Committee of Baotou Medical College (Institutional Review Board [IRB] No.002). $NaAsO_2$-treated mice were separated into four groups (n = 12 per group), including (1) 0 ppm $NaAsO_2$ group, (2) 0.5 ppm $NaAsO_2$ group, (3) 5 ppm $NaAsO_2$ group, (4) 50 ppm $NaAsO_2$ group. $NaAsO_2$ (Sigma-Aldrich, Shanghai, China, CAT#S7400) was administered via drinking water with an exposure duration of 48 weeks.

Animal euthanasia

Since it was necessary to collect total cerebrum in this study, the mice were euthanized at the end of the experimental period. All mice were sacrificed using an intraperitoneal injection of 1% pentobarbital sodium (Sigma-Aldrich, Shanghai, China, CAT#P3761) at a dose of 40 mg/kg. The body weight of each group of mice was recorded before euthanization.

H&E staining

The fixed brain tissues were washed with running water, dehydrated with gradient alcohol (Yongda Chemical, Tianjin, China, CAT#1001-0993), and embedded. The samples were cut into 3 μm thick paraffin slices and incubated at 65 ℃ for 4.5 h. Use the H&E staining kit (Baso, Zhuhai, China) to dewax, hydrate, rinse, and stain the sections. Sections were examined using a fluorescent microscope (BX43, OLYMPUS, Japan).

Nissl staining

Brain tissues were embedded in liquid paraffin, and sections were obtained at 3–5 μmol thickness. Xylene (Yongda Chemical, Tianjin, China, CAT#1330-20-7) was employed for dewaxing, and alcohol was used for rehydration. The brain tissues were stained with Nissl stain (Solarbio, Beijing, China, CAT#G1436) and randomly examined by pathologists.

TUNEL

Brain tissues underwent paraffin embedding and sectioning. Proteinase K (BOSTER, Wuhan, China, CAT#AR0056) was used to treat tissues at 37°C for 20 min and washed three times with PBS (Gibco, New York, USA, CAT#10010023). TUNEL (Beyotime, Shanghai, China, CAT#C1086) staining was carried out following the instructions of the TUNEL Apoptosis Detection Kit (Beyotime Biotechnology, Shanghai, China). The fluorescence signals were characterized utilizing a fluorescence microscope (BX43, OLYMPUS, Japan).

Real-time fluorescence quantitative PCR (RT-qPCR)

Adhering to the manual, total RNA was isolated from HT22 cells with TRIzol (TransGen Biotech, Beijing, China, CAT#ER511-01). Moreover, total RNA quality and quantity were investigated utilizing a NanoDrop (ThermoFisher Scientific, Waltham, USA). After RNA harvest, it was reverse transcribed using a Veriti Thermal Cycler (Applied Biosystems, USA, CAT# A48141). Real-time quantitative PCR (qPCR) was conducted using GoTaq® qPCR Master Mix (Promega, Madison, USA, CAT#A6001), utilizing U6 as internal controls. Primers used in this study were synthesized by Sangon Biotech (Shanghai) Co., Ltd. Primers utilized in this study were: miR-27a-3p: TCCACAGTGGCTAAGTTCCGC, GCGCTAGCACCATTTGAAATCAGTGTT, and U6: CTCG CTTCGGCAGCACATATACT, ACGCTTCACGAATTTGCGTGTC.qPCR reactions were all conducted using three replicates, and gene expression fold changes were computed using the $2^{-\Delta\Delta Ct}$ method.

Culture of mouse hippocampal HT22 cells and experimental groups

Cells were obtained from Preicella (Wuhan, China). Cultures were kept at a concentration of 5×10^5 cells/mL in DMEM (VivaCell, Shanghai, China, CAT#C3103-0500) alongside 10% fetal bovine serum (FBS, Servicebio, Wuhan, China, CAT#G8003), Penicillin–Streptomycin Solution (Gibco, New York, USA, CAT# 15070063) at 37 °C under humid conditions with 5% CO_2. The cells were split when they reached 70% to 90% confluence. The growth media was replenished every two days, and the arsenic group was exposed to a concentration of 6 μmol/L for 24 h. The concentration was selected based on preliminary cytotoxicity assays using the CCK-8 method[19].

Cell viability assessment

Cell viability was assessed using the Cell Counting Kit-8 (CCK-8) (Biosharp, Hefei, China, Cat# BS350A). HT22 cells were cultured in 96-well plates (with 5000 cells in each well) alongside dissolved $NaAsO_2$ (0, 2, 4, 6, 8, 10, and 12 μmol/L)for 24 h. CCK-8 reagent (10 μL) was added to each well, followed by incubation at 37 °C for 2 h.

Subsequently, the absorbance was measured at 450 nm using a microplate reader (BioTek Instruments). The cell survival rate (%) = (OD experimental – OD blank)/(OD control – OD blank) × 100%.

Transient cell transfection

HT22 cells underwent transfection using miR-27a-3p mimic (micrON mmu-miR-27a-3p mimic, Cat# miR10000537-1-5, Ribobio), or a corresponding scrambled control (micrON miRNA mimic Ncontrol #22, Cat# siN0000001-1-5, Ribobio) with Lipofectamine 2000 (Invitrogen, Waltham, USA CAT#11668500) adhering to the manufacturer's directions. Upregulation of miR-27a-3p was examined via RT-PCR 6 h following the transfection took place.

Transfections were conducted in 6-well plates using 7.5 μL Lipofectamine 2000 in 100 μL OptiMEM (1×) Medium per well. The mimics were diluted in 100 μL OptiMEM (1×, Gibco, CAT# 31985070) Medium per well. Following dilution, the miR-27a-3p mimic (6 μmol/L) was combined with diluted Lipofectamine 2000 Reagent (1:1) and then maintained for 5 min at room temperature. After transfection, the complex was mixed with HT22 cells in 1787.5 μL Opti-MEM (1 X) Medium and incubated for 6 h. Following the 6-h incubation, the cells were then incubated with sodium arsenite solution for 24 h, and collected for further experiments.

Apoptosis assay

As indicated by the manufacturer, Annexin V FITC/PI staining flow cytometry was utilized to examine apoptosis of HT22 cells. The cells were harvested in centrifuge tubes, and resuspended in cool PBS (1×) (Gibco, New York, USA, CAT#10010023) twice at 800 rpm for 4 min, removing the supernatant each time. Cells were then resuspended with 200 μL of Binding Buffer, 2 μL Annexin-V-FITC, and 2 μL PI (Transgen Biotech, Beijing, China, CAT#FA101-01) and were maintained in the absence of light at room temperature for 15 min, followed by apoptosis characterization by CytoFLEX flow cytometry (Beckman Coulter, Brea, USA).

Western blot

The concentration of proteins was examined using a BCA kit (Applygen, Beijing, China, CAT#P1511). Equal concentrations of protein were electrophoresed using SDS acrylamide gels. Protein bands were transferred onto PVDF membranes. The membranes were washed three times with TBST (Servicebio, CAT#G0004) for 10 min each, then blocked with 5% non-fat milk in TBST for 1 h at room temperature on a shaker and incubated with primary antibodies (Signalway Antibod, Maryland, USA) at 4 °C overnight. These antibodies encompassed anti-FTO (1:1000, CAT# 12749, SAB, Maryland, USA), anti-DRP1 (1:1000, CAT# 40853, SAB), anti-p-DRP1 (Ser616) (1:1000, CAT# 53847, SAB), anti-Bax (1:1000, CAT#BS0127R, BIOSS, Beijing, China), anti-Bcl-2 (1:1000, CAT# BSM33411M, BIOSS), or anti-Cleaved-caspase 3 (1:800, CAT#BS0081R, BIOSS). The rinsed membranes were maintained for 1 h with HRP-labelled goat anti-mouse secondary antibody (1:5000, CAT#ZB2305, ZSGB, Beijing, China). Visualization of bands was undertaken and positive protein signals on membranes were captured by an enhanced chemiluminescence light method (The company). β-actin (1:6000, CAT#AF7018, Affinity, USA) was employed as a standard. Data analysis was performed using Image J (NIH, USA).

Mitochondrial membrane potential assay

We investigated MMP activity in HT22 cells using the JC-1 probe (Beyotime Biotechnology, Shanghai, China, CAT#C2006). Cells were mixed with JC-1 (2 μM) and incubated at 37 °C for 30 min. To characterize HT22 MMP, fluorescence microscopy measured alterations in JC-1-associated fluorescence ranging from red (J-aggregates) to green (monomeric). The fluorescence intensity was examined using Image J (NIH, USA) to investigate the differences in MMP.

Statistical analysis

Unless otherwise stated, all data are presented as the mean and standard deviations (SDs). GraphPad Prism 9.0 was employed to produce graphics and assess statistical data. Variations between $NaAsO_2$ exposed and control groups were differentiated through one-way ANOVA. $p < 0.05$ represents statistical significance. At least three independent replications were performed for each experiment.

Results

Chronic exposure of mice to $NaAsO_2$ induces apoptosis of hippocampus

To investigate the effects of sodium arsenite on neuronal damage and apoptosis, we collected brain tissues from C57BL/6J mice treated with various concentrations of sodium arsenite and subjected them to H&E, TUNEL, and Nissl staining, respectively. In histopathological analysis, diffuse nuclear pycnosis, hyperstaining, and neuronal vacuolation were increased following $NaAsO_2$ exposure relative to the control group, as indicated by H&E staining. In contrast to the control group, the $NaAsO_2$ exposure group showed higher levels of TUNEL-positive and apoptotic neuronal cells. Histopathological analysis revealed that neuronal damage and apoptosis were most pronounced in the CA1 subregion of the hippocampus following chronic $NaAsO_2$ exposure (Fig. 1A–C).

Overexpression of miR-27a-3p alleviates $NaAsO_2$-induced cell death in HT22 cells

To investigate the role of miR-27a-3p in sodium arsenite-induced neuronal damage, we established an in vitro model by treating HT22 cells with sodium arsenite and miR-27a-3p mimics. The results showed that sodium arsenite treatment significantly reduced cell viability and miR-27a-3p expression levels in HT22 cells, whereas treatment with miR-27a-3p mimics effectively reversed these effects (Fig. 2A,B). These data indicate that sodium arsenite decreases HT22 cell viability, while miR-27a-3p overexpression can counteract this process.

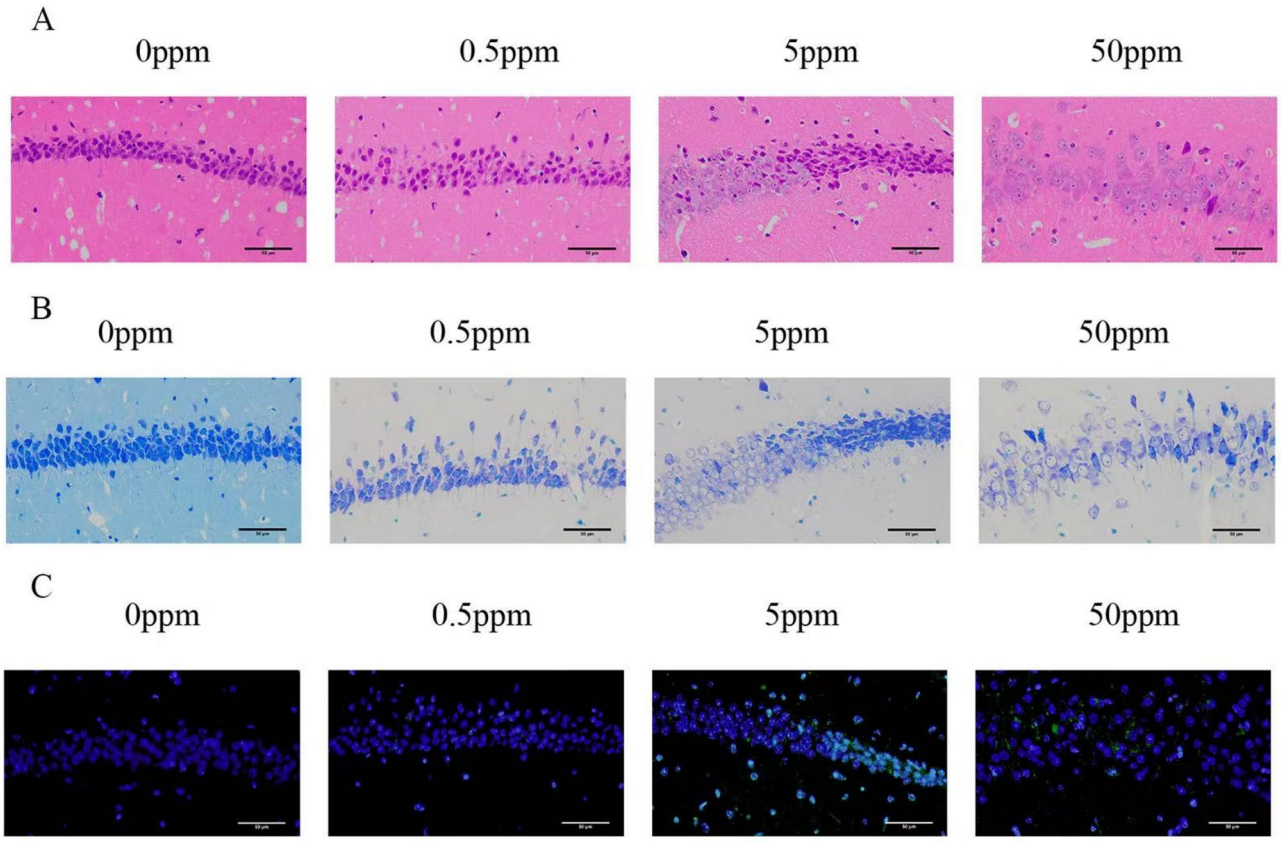

Fig. 1. Chronic exposure of mice to $NaAsO_2$ induce apoptosis of hippocampus. Mice were exposed to $NaAsO_2$ (0, 0.5, 5 or 50 ppm) in drinking water for 48 weeks. (**A**) H&E staining conducted for monitoring histomorphologic features of brain tissue. (**B**) The levels of TUNEL-positive cells with TUNEL levels. (**C**) The number of apoptotic neurons observed with Nissl staining. Data are presented as mean ± SD, n = 3. $^*p < 0.05$, treatment group versus the control mice.

MiR-27a-3p via FTO/DRP1 axis overcomes the damage in $NaAsO_2$-treated HT22 cells

The gene specifically tuned by miR-27a-3p was examined using the NCBI online tools. FTO is a possible position of action for miR-27a-3p (Fig. 3A). Western blot was performed to investigate the mechanisms $NaAsO_2$ uses to regulate apoptosis in vitro. The expression of FTO, DRP1, and p-DRP1 (Ser616) in HT22 cells was elevated by $NaAsO_2$ treatment. However, this impact was inhibited when miR-27a-3p mimics were present (Fig. 3B–E). These findings suggest that apoptosis induction in HT22 cells by $NaAsO_2$ is mediated by activating the FTO/DRP1 pathway, which can be overcome by miR-27a-3p.

MiR-27a-3p inhibits apoptosis in $NaAsO_2$-treated HT22 cells via the FTO/DRP1 axis

We employed flow cytometry to identify apoptosis and found that HT22 cells experienced significantly increased apoptosis upon exposure to $NaAsO_2$ (Fig. 4A,B). Similar to the observed increase in apoptosis, $NaAsO_2$ produced a notable increase in active Bax and Cleaved-caspase 3, both pro-apoptotic enzymes (Fig. 4C,E,F). In contrast, $NaAsO_2$ produced a considerable reduction in anti-apoptotic protein (Bcl-2) levels in HT22 cells (Fig. 4C,D). However, when miR-27a-3p mimics were introduced, these impacts were reversed (Fig. 4A–F).

MiR-27a-3p inhibits MMP levels in $NaAsO_2$-treated HT22 cells via the FTO/DRP1 axis

Utilizing a fluorescence microscope to characterize MMP levels in HT22 cells, we identified that $NaAsO_2$ significantly lowered MMP levels (Fig. 5A,B). Again, the influence was overcome upon exposure to miR-27a-3p mimics (Fig. 5A,B). Therefore, introducing miR-27a-3p effectively mitigates $NaAsO_2$-associated damage to mitochondria in HT22 cells.

Discussion

Globally, arsenic exposure causes significant health problems and is a global public health concern[20]. The association between environmental arsenic exposure and nerve damage is becoming more evident with studies demonstrating that hippocampal neurons can undergo apoptosis as a result of prolonged arsenic exposure[21]. Arsenic exposure can lead to neurotoxicity by triggering apoptosis, but the exact mechanism is unknown. The hippocampus, a brain region sensitive to dysfunctional transition metal homeostasis, plays critical roles in

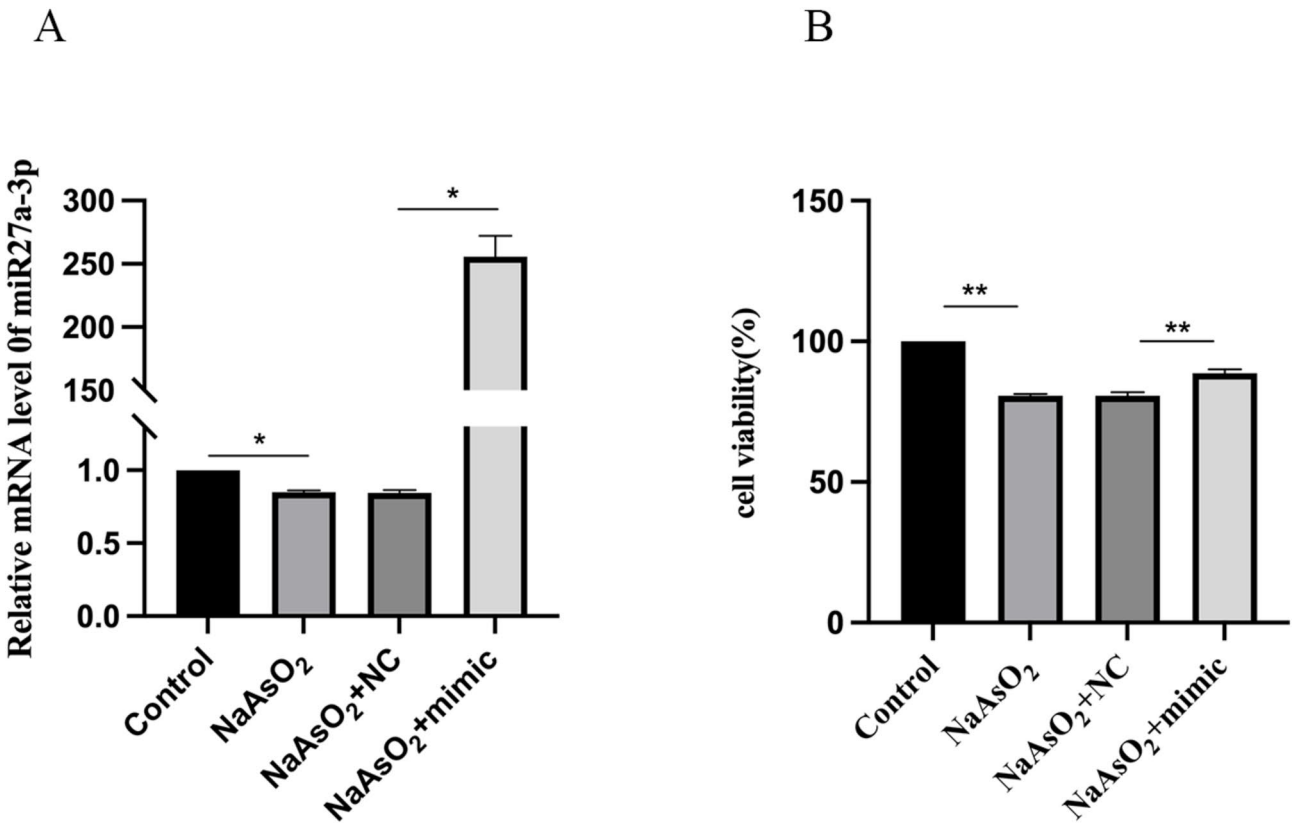

Fig. 2. $NaAsO_2$ induce decrease of miR-27a-3p levels, inhibition of miR-27a-3p increase the cell viability in $NaAsO_2$-treated HT22 cells. HT22 cells were treated with 0 or 50 nM miR-27a-3p mimic/NC for 6 h, then exposed to 0 or 6 μmol $NaAsO_2$ for 24 h. (**A**) Production of miR-27a-3p in HT22 cells (mean ± SD, n = 3). (**B**) HT22 cells examined using CCK-8 (mean ± SD, n = 3). *$p < 0.05$, ** $p < 0.01$ vs. Control or $NaAsO_2$ + NC.

learning, memory formation, emotion regulation, and pain perception. Neurodegenerative diseases are closely associated with damaged hippocampal structure and function[22]. The in vivo findings of this study demonstrated that the administration of $NaAsO_2$-induced histopathological alterations in hippocampal tissue and triggered apoptosis in hippocampal cells among C57BL/6J mice. MiRNAs play a crucial role in the progression of apoptosis[4,23]. The study conducted by Chi B et al. demonstrated that elevated levels of miRNA-26a were associated with enhanced neuronal apoptosis in the brain[24]. The overexpression of miRNA-23a-3p rescued cardiomyocytes from apoptosis induced by high glucose[25]. The level of miR-27a-3p was significantly decreased in HT22 cells exposed to $NaAsO_2$ as detected by qRT-PCR. Our in vitro assessments suggested that apoptosis was enhanced in the $NaAsO_2$-exposed mice. We found that sodium arsenite induced apoptosis in HT22 cells and that miR-27a-3p mimics slowed down the process. According to these findings, miR-27a-3p may contribute to neuronal injury and apoptosis induced by $NaAsO_2$. Our examination explored the possible impact of miR-27a-3p on $NaAsO_2$-induced cell death and highlighted its suppressive effect. A recent study uncovered that reducing miR-27a-3p levels enhanced cell development, Lactate Dehydrogenase (LDH) release, inflammation, and apoptosis caused by $NaAsO_2$ via Nuclear Receptor Interacting Protein 1 (NRIP1) targeting[26]. This suggests that the diverse functions of miR-27a-3p may contribute to its overall impact.

Traditionally, miRNAs exercise their influence by inhibiting the production of specific genes[27]. In this study, we predicted and screened potential target genes of miR-27a-3p by reviewing the literature and using the bioinformatics database NCBI, and predicted that HT22 cells would undergo apoptosis as a result of $NaAsO_2$-induced miR-27a-3p/FTO/DRP1 signaling. By activating its s616 phosphorylation level, DRP1 (Ser616) regulates mitochondrial fission and mitochondria-mediated endogenous apoptosis by up-regulating mitochondrial fission. FTO is produced in neurons across the brain, transiting between the nucleus and cytoplasm[28]. It functions in diverse biological processes and cell death, likely involved in apoptosis[29]. Through activation of the Protein Kinase B/Nuclear factor erythroid 2-related factor 2 (AKT/Nrf2) pathway, overexpression of FTO alleviates Cadmium (Cd)-induced cell death and oxidative damage in granulosa cells[30]. Another study indicated that FTO inhibitors protect dopamine neurons from cell death produced by growth factor limitation[31]. These studies indicate that FTO expression is unstable in apoptosis. Our findings demonstrate that miR-27a-3p promotes FTO/DRP1 signaling, while the miR-27a-3p mimics exhibited an apparent reversal effect. The results of this study are consistent with the above findings. FTO concentrations were suppressed by miR-27a-3p mimics, indicating that it inhibits $NaAsO_2$-induced apoptosis progression through its excitatory effect on FTO/DRP1 signaling. In contrast, DRP1 promotes mitochondrial fission in healthy cells to maintain homeostasis, mediating

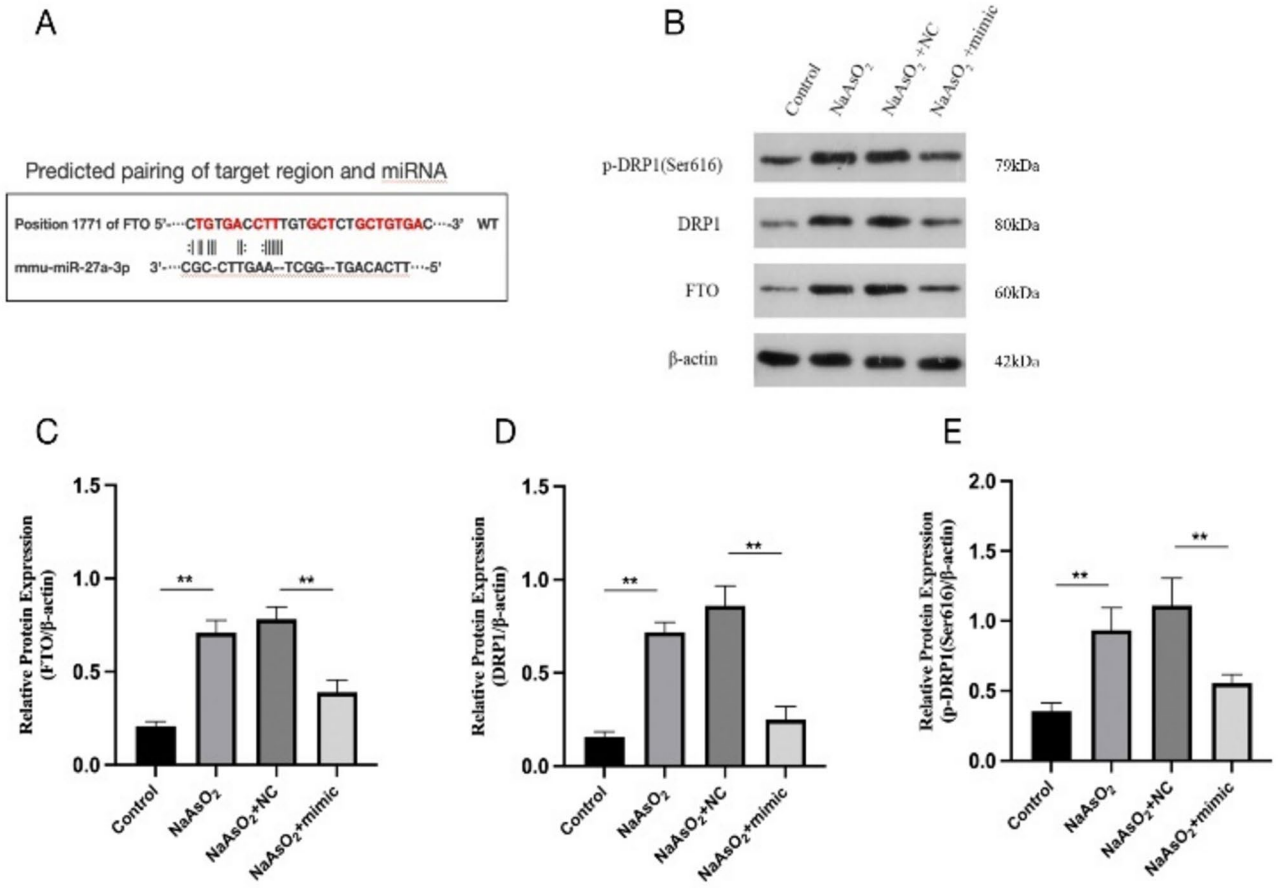

Fig. 3. MiR-27a-3p via FTO/DRP1 axis overcomes the damage in $NaAsO_2$-treated HT22 cells. HT22 cells were treated with 0 or 50 nM miR-27a-3p mimic/NC for 30 min, then exposed to 0 or 6 μmol $NaAsO_2$ for 24 h. (**A**) The genetic arrangement of FTO at position 1771 indicates a putative binding location for miR-27a-3p within its 3′ UTR. (**B**) Western blot indicating expression of FTO, DRP1, and p-DRP1 (Ser616) in HT22 cells. Membranes were cut horizontally prior to hybridization with antibodies. Full-length blots are presented in Supplementary Information. (**C**–**E**) Comparative production of FTO (**C**), DRP1 (**D**), and p-DRP1 (Ser616) (**E**), compared to β-actin (mean ± SD, n = 3). $^{**}p < 0.01$ vs. Control or $NaAsO_2$ + NC.

mitochondrial fragmentation in apoptotic cells[32]. The levels of DRP1 and mitochondrial impairment were significantly elevated in both human Osteoarthritis (OA) cartilage and mouse joints undergoing Destabilization of the Medial Meniscus (DMM) surgery, exhibiting elevated chondrocyte apoptosis[33]. In this study, sodium arsenite-induced activation of the FTO/DRP1 signaling pathway triggered apoptosis in HT22 cells, an effect that was reversed by miR-27a-3p overexpression.

It has been widely reported that the mitochondrial apoptotic pathway is one of the major mechanisms of apoptosis. This process decreases the mitochondrial membrane potential and ultimately leads to cell death[34]. Proteins such as Bax, Bcl-2, and cleaved caspase 3 serve as critical markers of apoptosis and are involved in triggering the apoptotic process. According to the results of this experiment, HT22 cells treated with $NaAsO_2$+ mimic showed increased levels of Bcl-2 expression and decreased levels of Bax and cleaved caspase 3 expression compared with the sodium arsenite-exposed group. This suggests that up-regulation of miR-27a-3p expression level in HT22 cells can effectively inhibit 6 mol/L $NaAsO_2$-induced apoptosis. In order to investigate whether sodium arsenite-induced apoptosis in HT22 cells was related to miR-27a-3p-mediated mitochondrial damage, the cellular mitochondrial membrane potential was detected in this study by using JC-1 probe and fluorescence microscopy, The mitochondrial membrane potential of cells in the sodium arsenite-treated group was decreased, and this process was reversed after transfection with miR-27a-3p mimic. Overall, it was demonstrated that miR-27a-3p was involved in reversing mitochondrial damage and apoptosis induced by $NaAsO_2$ in HT22 cells, suggesting that miR-27a-3p may be able to regulate endogenous mitochondrial pathways that mediate apoptosis in HT22 cells.

In this study, we focused on the role and underlying mechanisms of miR-27a-3p in $NaAsO_2$-induced apoptosis in HT22 cells. In addition to miR-27a-3p, other miRNAs have been reported to modulate cell viability in response to environmental neurotoxicants. For instance, miR-206 exerts its effects on methylmercury-induced neurotoxicity by modulating the REST/HDAC4/Sp1/Sp4/BDNF axis[35]. Moreover, studies have shown that miRNAs such as miR-124 and miR-137 influence neuronal survival and function by regulating apoptosis-related

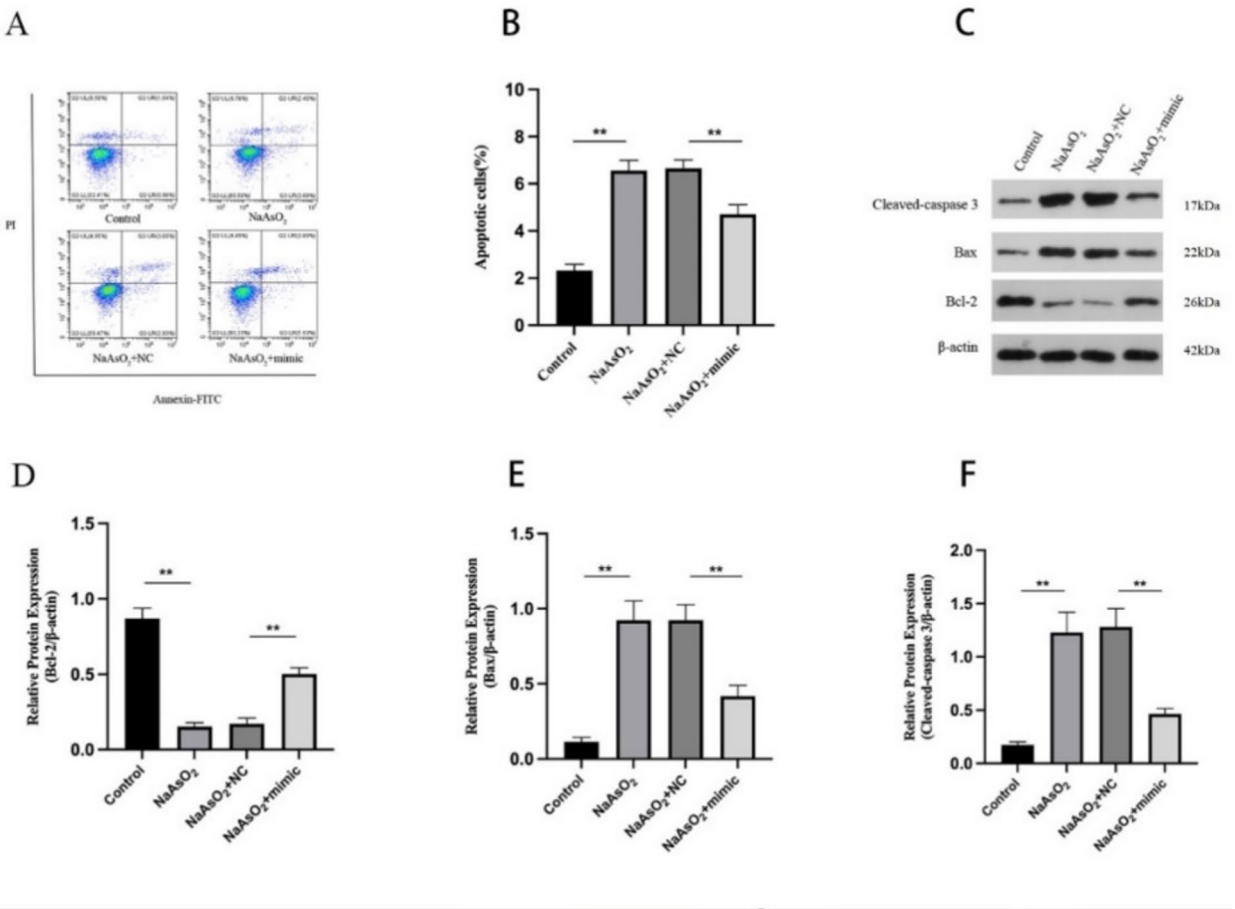

Fig. 4. MiR-27a-3p inhibits apoptosis in $NaAsO_2$-treated HT22 cells via the FTO/DRP1 axis. (**A**) Flow cytometry examination of apoptosis. (**B**) Apoptotic rate in HT22 cells (mean ± SD, n = 3). (**C**) Western blot of Bcl-2, Bax, and Cleaved-caspase 3 in HT22 cells. Membranes were cut horizontally prior to hybridization with antibodies. Full-length blots are presented in Supplementary Information. (**D**–**F**) Comparative expression levels of Bcl-2, Bax, and Cleaved-caspase 3 standardized to β-actin (mean ± SD, n = 3). $^{**}p < 0.01$ vs. Control or $NaAsO_2$ + NC.

pathways during neurotoxic processes[36]. Beyond miRNA-mediated regulation, environmental neurotoxicants like $CuCl_2$ can also induce neuronal apoptosis through epigenetic mechanisms[37]. These findings collectively highlight the complexity of neurotoxicity, involving both miRNA networks and epigenetic modifications triggered by diverse toxic agents.

In our study, miR-27a-3p attenuated the $NaAsO_2$-induced apoptotic process in HT22 cells by targeting FTO to inhibit the FTO/DRP1 signaling pathway. This finding further validates the regulatory role of miRNAs in neurotoxicity and provides a new direction for future research. Future work could explore the mechanism of action of other miRNAs in environmental neurotoxicant-induced neurotoxicity, as well as their potential synergistic or antagonistic effects with miR-27a-3p. This will contribute to a more comprehensive understanding of miRNA regulatory networks in neurotoxicity and provide a theoretical basis for the development of miRNA-based therapeutic strategies. However, our current findings are derived from experiments conducted in hippocampal HT22 cells, which are a well-established model for studying hippocampal neuronal responses. While this study highlights the role of miR-27a-3p/FTO/DRP1 signaling in arsenic-induced apoptosis within hippocampal neurons, whether this pathway is activated in cortical neurons remains to be explored. Future work should extend these findings to cortical neuronal models to assess pathway specificity and broader applicability.

Conclusions

Briefly, arsenic exposure decreases neuronal mitochondrial membrane potential through miR-27a-3p modulation of the FTO/DRP1 signaling pathway, which induces HT22 apoptosis and leads to hippocampal neuronal damage (Fig. 6).

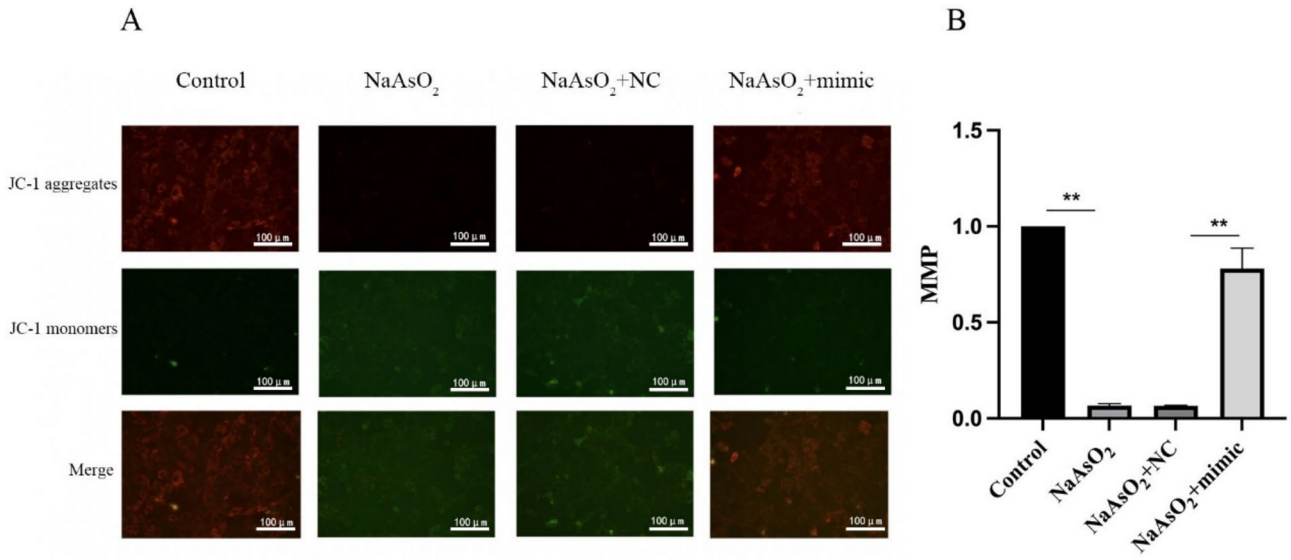

Fig. 5. MiR-27a-3p inhibits MMP levels in $NaAsO_2$-treated HT22 cells via the FTO/DRP1 axis. HT22 cells were treated with 0 or 50 nM miR-27a-3p mimic/NC for 30 min, then exposed to 0 or 6 μmol $NaAsO_2$ for 24 h. (**A**) Fluorescence examination of MMP levels in HT22 cells. (**B**) The levels of MMP (mean ± SD, n = 3). $^{**}p < 0.01$ vs. Control or $NaAsO_2$ + NC.

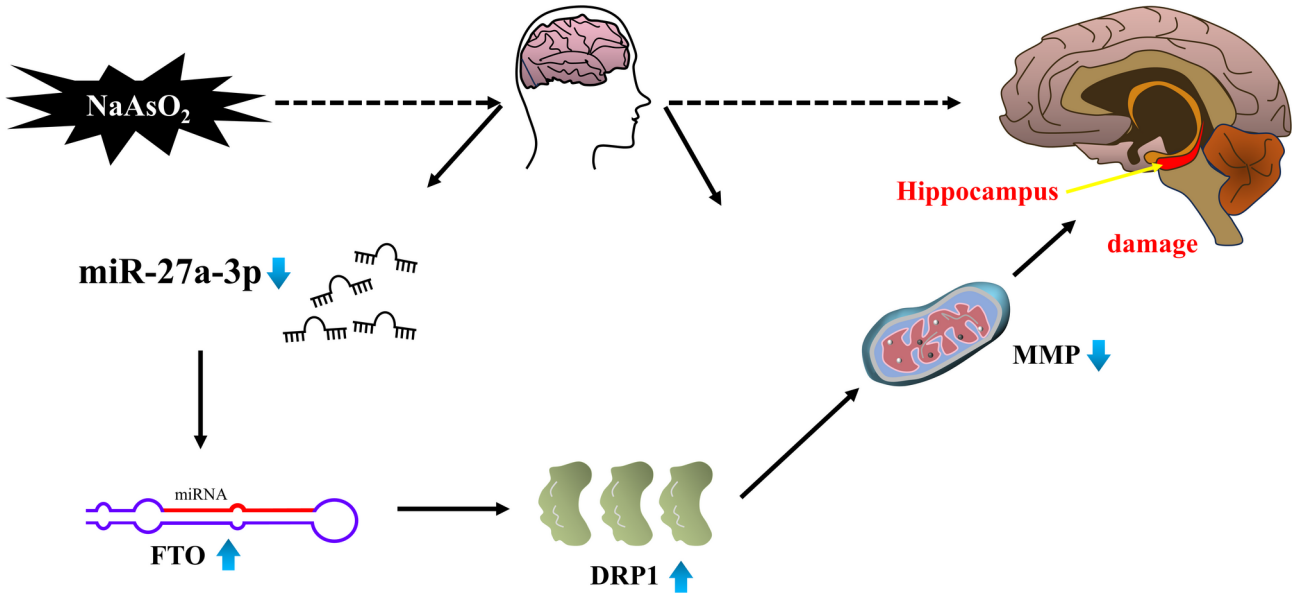

Fig. 6. MiR-27a-3p via FTO is involved in arsenite-induced apoptosis of HT22 cells (Figure was created by Zhao Siqi using PowerPoint).

Data availability

All data are available from the corresponding author upon a reasonable request.

Received: 26 November 2024; Accepted: 17 April 2025
Published online: 23 April 2025

References

1. Negi, V., Singh, P., Singh, L., Pandey, R. K. & Kumar, S. A comprehensive review on molecular mechanism involved in arsenic trioxide mediated cerebral neurodegenerative and infectious diseases. *Infect. Disord. Drug Targets* **24**, e131123223549 (2024).
2. Mochizuki, H. Arsenic neurotoxicity in humans. *Int. J. Mol. Sci.* **20**, 3418 (2019).
3. Najafi, N. et al. Melatonin attenuates arsenic-induced neurotoxicity in rats through the regulation of miR-34a/miR-144 in Sirt1/Nrf2 pathway. *Biol. Trace Elem. Res.* **202**, 3163–3179 (2024).

4. Rezaee, D. et al. The role of microRNAs in the pathophysiology of human central nervous system: A focus on neurodegenerative diseases. *Ageing Res. Rev.* **92**, 102090 (2023).
5. Li, S., Lei, Z. & Sun, T. The role of microRNAs in neurodegenerative diseases: A review. *Cell Biol. Toxicol.* **39**, 53–83 (2023).
6. Lu, J., Zhou, N., Yang, P., Deng, L. & Liu, G. MicroRNA-27a-3p downregulation inhibits inflammatory response and hippocampal neuronal cell apoptosis by upregulating mitogen-activated protein kinase 4 (MAP2K4) expression in epilepsy: In vivo and in vitro studies. *Med. Sci. Monit.* **25**, 8499–8508 (2019).
7. Ma, M., Yin, Z., Zhong, H., Liang, T. & Guo, L. Analysis of the expression, function, and evolution of miR-27 isoforms and their responses in metabolic processes. *Genomics* **111**, 1249–1257 (2019).
8. Chen, L. et al. Extracellular vesicles carry miR-27a-3p to promote drug resistance of glioblastoma to temozolomide by targeting BTG2. *Cancer Chemother. Pharmacol.* **89**, 217–229 (2022).
9. Luo, J. et al. MicroRNA-27a-3p relieves inflammation and neurologic impairment after cerebral ischaemia reperfusion via inhibiting lipopolysaccharide induced TNF factor and the TLR4/NF-κB pathway. *Eur. J. Neurosci.* **56**, 4013–4030 (2022).
10. Lv, X. et al. MicroRNA-27a-3p suppression of peroxisome proliferator-activated receptor-γ contributes to cognitive impairments resulting from sevoflurane treatment. *J. Neurochem.* **143**, 306–319 (2017).
11. Zhang, Z., He, J. & Wang, B. Circular RNA circ_HECTD1 regulates cell injury after cerebral infarction by miR-27a-3p/FSTL1 axis. *Cell Cycle* **20**, 914–926 (2021).
12. Li, W., Zhu, Q., Xu, X. & Hu, X. MiR-27a-3p suppresses cerebral ischemia-reperfusion injury by targeting FOXO1. *Aging (Albany NY)* **13**, 11727–11737 (2021).
13. Tichanek, F. et al. Hippocampal mitochondrial dysfunction and psychiatric-relevant behavioral deficits in spinocerebellar ataxia 1 mouse model. *Sci. Rep.* **10**, 5418 (2020).
14. Misrani, A., Tabassum, S., Zhang, Z.-Y., Tan, S.-H. & Long, C. Urolithin A prevents sleep-deprivation-induced neuroinflammation and mitochondrial dysfunction in young and aged mice. *Mol .Neurobiol.* **61**, 1448–1466 (2024).
15. Firdaus, F. et al. Evaluation of phyto-medicinal efficacy of thymoquinone against Arsenic induced mitochondrial dysfunction and cytotoxicity in SH-SY5Y cells. *Phytomedicine* **54**, 224–230 (2019).
16. Pan, T. et al. The role m6A RNA methylation is CNS development and glioma pathogenesis. *Mol. Brain* **14**, 119 (2021).
17. Wang, Q.-S. et al. Bone marrow mesenchymal stem cell-derived exosomal KLF4 alleviated ischemic stroke through inhibiting N6-methyladenosine modification level of Drp1 by targeting lncRNA-ZFAS1. *Mol. Neurobiol.* **60**, 3945–3962 (2023).
18. Du, P. et al. The miR-27a-3p/FTO axis modifies hypoxia-induced malignant behaviors of glioma cells. *Acta Biochim. Biophys. Sin. (Shanghai)* **55**, 103–116 (2023).
19. Zhang, Q. et al. Study on the mechanism of FTO/DRP1 signaling pathway in arsenic-induced mitochondrial apoptosis in HT22 cells. *Ind. Hyg. Occup. Dis.* **50**(3), 225–232 (2024).
20. Frisbie, S. H. & Mitchell, E. J. Arsenic in drinking water: An analysis of global drinking water regulations and recommendations for updates to protect public health. *PLoS One* **17**, e0263505 (2022).
21. Chen, Y. et al. Arsenic induced autophagy-dependent apoptosis in hippocampal neurons via AMPK/mTOR signaling pathway. *Food Chem. Toxicol.* **179**, 113954 (2023).
22. Chen, Y., Cao, P., Xiao, Z. & Ruan, Z. m(6)A methyltransferase METTL3 relieves cognitive impairment of hyperuricemia mice via inactivating MyD88/NF-κB pathway mediated NLRP3-ASC-Caspase1 inflammasome. *Int. Immunopharmacol.* **113**, 109375 (2022).
23. Ma, Y.-M. & Zhao, L. Mechanism and therapeutic prospect of miRNAs in neurodegenerative diseases. *Behav. Neurol.* **2023**, 8537296 (2023).
24. Chi, B. et al. Upregulation of miRNA-26a enhances the apoptosis of cerebral neurons by targeting EphA2 and inhibiting the MAPK pathway. *Dev. Neurosci.* **44**, 615–628 (2022).
25. Wu, F. et al. Upregulation of miRNA-23a-3p rescues high glucose-induced cell apoptosis and proliferation inhibition in cardiomyocytes. *In Vitro Cell Dev. Biol. Anim.* **56**, 866–877 (2020).
26. Ren, X. & Zhou, X. Circ_0000011 promotes cerebral ischemia/reperfusion injury via miR-27a-3p-dependent regulation of NRIP1. *Metab. Brain Dis.* **38**, 295–306 (2023).
27. Zhang, H. et al. Investigation of key miRNAs and their target genes involved in cell apoptosis during intervertebral disc degeneration development using bioinformatics methods. *J. Neurosurg. Sci.* **66**, 125–132 (2022).
28. Aas, A. et al. Nucleocytoplasmic shuttling of FTO does not affect starvation-induced autophagy. *PLoS One* **12**, e0168182 (2017).
29. Tian, M.-Q. et al. The increase of Nrf2 m6A modification induced by FTO downregulation promotes hippocampal neuron injury and aggravates the progression of epilepsy in a rat model. *Synapse* **77**, e22270 (2023).
30. Ding, H. et al. FTO alleviates $CdCl_2$-induced apoptosis and oxidative stress via the AKT/Nrf2 pathway in bovine granulosa cells. *Int. J. Mol. Sci.* **23**, 4948 (2022).
31. Selberg, S. et al. Small-molecule inhibitors of the RNA M6A demethylases FTO potently support the survival of dopamine neurons. *Int. J. Mol. Sci.* **22**, 4537 (2021).
32. Jenner, A. et al. DRP1 interacts directly with BAX to induce its activation and apoptosis. *EMBO J.* **41**, e108587 (2022).
33. Ansari, M. Y., Novak, K. & Haqqi, T. M. ERK1/2-mediated activation of DRP1 regulates mitochondrial dynamics and apoptosis in chondrocytes. *Osteoarthr. Cartil.* **30**, 315–328 (2022).
34. Lim, J., Bang, Y., Kim, K.-M. & Choi, H. J. Differentiated HT22 cells as a novel model for in vitro screening of serotonin reuptake inhibitors. *Front. Pharmacol.* **13**, 1062650 (2022).
35. Guida, N. et al. The miR206-JunD circuit mediates the neurotoxic effect of methylmercury in cortical neurons. *Toxicol. Sci.* **163**(2), 569–578 (2018).
36. Sun, H., Li, J. J., Feng, Z. R., Liu, H. Y. & Meng, A. G. MicroRNA-124 regulates cell pyroptosis during cerebral ischemia-reperfusion injury by regulating STAT3. *Exp. Ther. Med.* **20**(6), 227 (2020).
37. Ruggiero, S. et al. Sp4/HD11 and Sp1/HAT-p300 complexes induce apoptotic cell death in $CuCl_2$-treated neurons by modulating histone acetylation on BCL-W and BAX promoters. *Neurochem. Int.* **186**, 105973 (2025).

Author contributions

Q.Z. and S.Z.: design, data analysis, and draft of the manuscript. T.M. and S.W.: investigation and formal analysis. Y.W. and S.X.: software and resources. X.W. and L.W.: manuscript revisions and grant application. All authors reviewed and consented to the publication of this manuscript version.

Funding

This work was supported by the National Natural Science Foundation of China (82060605).

Declarations

Competing interests

The authors declare no competing interests.

Ethics approval

This study was approved by the Experimental Animal Ethics Committee of Baotou Medical College (Institutional Review Board [IRB] No.002). All procedures were performed in accordance with the ethical standards of the Guide for the Care and Use of Laboratory Animals published by the National Institutes of Health, and ARRIVE guidelines.

Additional information

Supplementary Information The online version contains supplementary material available at https://doi.org/10.1038/s41598-025-99195-2.

Correspondence and requests for materials should be addressed to X.W. or L.W.

Reprints and permissions information is available at www.nature.com/reprints.

Publisher's note Springer Nature remains neutral with regard to jurisdictional claims in published maps and institutional affiliations.